Contribution from the Industrial Chemicals Division,
NL Industries, Inc., Hightstown, New Jersey 08520

Vibrational and Thermal Study of Antimony Oxides

C. A. CODY,* L. DiCARLO, and R. K. DARLINGTON

Received October 6, 1978

Antimony oxides have been characterized by combining thermogravimetric analysis and Raman spectroscopy. Residues and condensates produced from the thermogravimetric analysis of Sb_2O_3 (senarmontite and valentinite), Sb_2O_4 (α and β phase), $Sb_2O_5 \cdot XH_2O$, and Sb_6O_{13} were identified by X-ray diffraction and Raman and infrared spectroscopy. The formation of β-Sb_2O_4 was accomplished by heating α-Sb_2O_4 or Sb_6O_{13} in closed quartz capillaries at 960 °C. Heating the two polymorphs of Sb_2O_3 in air revealed that both senarmontite and valentinite exhibited simultaneous volatilization and oxidation; however, senarmontite displayed a net weight loss of 21–26% whereas valentinite gained 0.8–2.4%. TG experiments of $Sb_2O_5 \cdot XH_2O$ heated in air indicated that the 650–850 °C plateau was Sb_6O_{13} and the 890–970 °C plateau was α-Sb_2O_4. Infrared and Raman spectra of all the above mentioned antimony oxides were recorded, with the Raman spectra of α-Sb_2O_4, β-Sb_2O_4, and Sb_6O_{13} being reported for the first time.

Introduction

Antimony oxides are known to exist in several different compositions and display polymorphism. The two common forms of Sb_2O_3 are the cubic phase senarmontite and the orthorhombic phase valentinite.[1-3] The polymorphic forms of Sb_2O_4 are the orthorhombic α phase (cervantite) and a high-temperature monoclinic β phase.[4] Antimonic acid can be best described as $Sb_2O_5 \cdot XH_2O$, its dehydration and thermal decomposition product being Sb_6O_{13}, i.e., $Sb_2O_{4.35}$; further heating of Sb_6O_{13} yields Sb_2O_4 as the final composition.[5]

Numerous studies have discussed methods of preparation, description of physical properties, and the interconversion between the various polymorphs.[4-9] The results from these studies are not entirely consistent, however, making exact interpretations very difficult. For example, Waring et al.[9] concluded that β-Sb_2O_4 was the high-pressure form of Sb_2O_4 while Stewart et al.[5] reported production of β-Sb_2O_4 at atmospheric pressure by heating Sb_6O_{13} to 935 °C in air. The thermal analysis study of antimony oxides reported by Agrawal et al.[10] found that cubic Sb_2O_3 gained 4.5 wt % when heated in air up to 630 °C. Agrawal et al. also reported that on heating in N_2 or argon amospheres senarmontite (cubic) volatilized at 550 °C whereas valentinite (orthorhombic) remained stable up to 630 °C.

This investigation was undertaken to examine discrepancies in reported Sb_2O_3 chemistry and that observed in this work and to examine the thermal behavior of all the antimony oxides. By combining thermal analysis and Raman spectroscopic techniques, rapid and unique identification of all starting, intermediate, and final products was achieved. The Raman spectra of α-Sb_2O_4, β-Sb_2O_4, and Sb_6O_{13} are also reported for the first time, on phases which were identified from X-ray diffraction powder patterns.

Experimental Section

Samples of Sb_2O_3 were of high purity Red Star grade, produced by NL Industries. Samples of Sb_2O_4 and $Sb_2O_5 \cdot XH_2O$ were prepared from NL's Red Star Sb_2O_3. Samples of $Sb_2O_5 \cdot XH_2O$ were also purchased from ROC/RIC; both pentoxides were identical in chemical and physical behavior. All preparations were confirmed and identified by X-ray diffraction.

A DuPont 951 thermogravimetric analyzer, equipped with a dual pen thermal 990 programmer, was used to record the thermal behavior of each sample. Thermolysis curves were displayed as weight loss vs. temperature and as the first derivative of weight loss with respect to temperature. Dry air, nitrogen, or oxygen atmospheres could be maintained at ambient pressure in the unit.

Raman spectra were excited by a Coherent Radiation Model 52A argon ion laser. The exciting line was 4880 Å with ~300 mW of power at the sample. A few spectral runs were performed with the 5145-Å line to eliminate spurious emission lines or grating ghosts. The 90° scattered light was analyzed by a Spex 1401 double monochromator employing dc detection via an FW-130 photomultiplier. Spectral slits were 1 and 4 cm^{-1}; the monochromator was calibrated by scanning over emission lines of the laser. Samples were examined as packed powders in 2-mm i.d. glass or quartz capillaries. No polarization studies were undertaken.

X-ray powder diffraction patterns were recorded on a Philips X-ray diffractometer using Cu Kα radiation. Once verification of a sample's diffraction pattern to that found in the JCPDS powder diffraction file clearly established that a pure phase had been produced, Raman spectra were then recorded on that phase and used as reference spectra. This approach allowed rapid Raman identification of milligram-sized samples produced from the thermal runs, an important advantage over other techniques. Residues as well as condensates from thermogravimetric analysis were identified accurately and quickly on only a few milligrams, by this method.

Infrared spectra were recorded on a Perkin-Elmer Model 621 spectrophotometer from 1100 to 400 cm^{-1}. Samples were ground with mineral oil and spectra recorded of thin films on CsI windows.

Results and Discussion

By thermogravimetric (TG) analysis it was found that when senarmontite (cubic Sb_2O_3) is heated in air at 20 °C/min, volatilization of Sb_2O_3 and oxidation to Sb_2O_4 occur simultaneously. The net effect of the competing reaction is a 21% weight loss between 500 and 660 °C (Figure 1, trace a). Heating the remaining residue from 660 to 935 °C does not result in any further weight change and the final product is α-Sb_2O_4. The thermolysis curve produced by heating senarmontite in N_2 at 20 °C/min shows a two-stage decomposition (Figure 1, trace b); the first stage is associated with sublimation of senarmontite and the second stage is due to the volatilization of the melt.

When valentinite (orthorhombic Sb_2O_3) is heated in air at 20 °C/min, there is no weight loss up to 450 °C, there is a 0.2% weight loss between 450 and 540 °C, and there is an 0.8% weight gain from 550 to 780 °C (Figure 1, trace c). There is no further detectable weight change upon heating the residue to 935 °C; the final product is α-Sb_2O_4. A two-stage volatilization curve is produced when valentinite is heated in N_2; the first stage is due to the sublimation of valentinite, and the second stage is produced by the volatilization of the melt (Figure 1, trace d).

The rate and degree of volatilization and the simultaneous oxidation of Sb_2O_3 to Sb_2O_4 are minimally affected by particle size, surface area, heating rate, and method of preparation. For example, gains in weight from 0.8% (Figure 1, trace c) to 2.4% were recorded on different valentinite samples. Oxygen absorption resulting in a net gain in weight only occurs when valentinite is heated in air and does not occur when senarmontite is heated in air. Our findings clearly show a net loss (see Figure 1, trace a) on heating senarmontite in air. These results contradict the findings of Agrawal et al.,[10] who reported that senarmontite gained weight when heated in air.

0020-1669/79/1318-1572$01.00/0

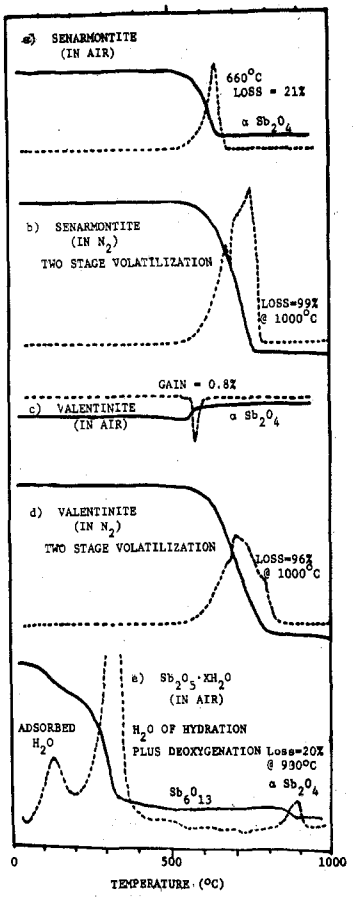

Figure 1. Thermolysis curves of various antimony oxides. Heating rates for traces a–d are 20 °C/min and the rate for trace e is 50 °C/min. Solid line denotes weight change. Dotted line represents the first derivative of the weight change.

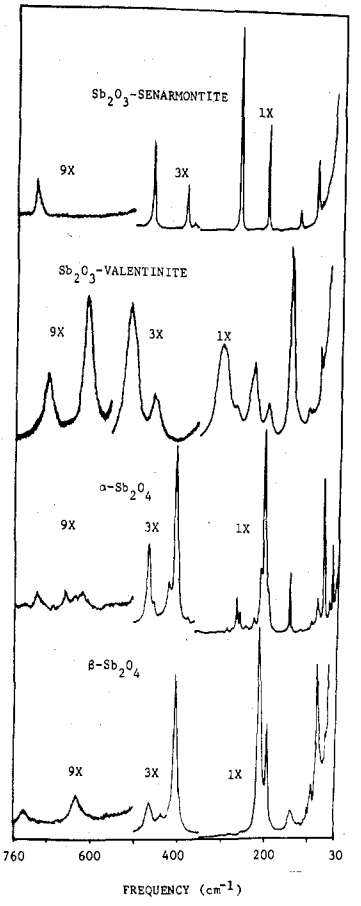

Figure 2. Raman spectra of polycrystalline senarmontite, valentinite, α-Sb_2O_4, and β-Sb_2O_4. Spectra were recorded at 1 cm^{-1} resolution.

No explanation can be given for Agrawal's observation of a weight gain. Repeats of their experimental conditions with well-characterized senarmontite samples always resulted in a weight loss.[11]

The infrared[12-13] and Raman[14] spectra of senarmontite and valentinite have been previously reported and interpreted. The frequencies observed in this study for the five antimony oxides are listed in Table I and are reported here for completeness. These results were also used to characterize the thermal behavior of the various antimony oxides. Raman spectra of the various antimony oxides are given in Figures 2 and 3.

Borgen and Krogh-Moe[12] have reported the infrared spectra of Sb_2O_3 glass. Their results indicated that the Sb_2O_3 glass had an infrared spectrum similar to senarmontite (cubic Sb_2O_3) and that the glass phase could be formed by pouring molten Sb_2O_3 into cold water. During the present investigation repeated attempts were made to form the glass by quenching the Sb_2O_3 melt with liquid nitrogen or ice water, but in each experiment the Raman spectrum of the quenched product was nearly identical with that of valentinite. Samples of senarmontite were also sealed in quartz capillaries, heated 100 °C above the melting point and quenched with ice water. Again, the final product was valentinite.

Several attempts were made to form the glass by slightly altering the stoichiometry of Sb_2O_3. Antimony metal was added to the melt in ~2 wt % excess; then the melt was stirred and quenched with ice water. The quenched product was again valentinite.

The Raman spectrum of the Sb_2O_3 melt (Figure 3) has many of the characteristic features found in the valentinite internal mode spectrum (Figure 2, 400–800 cm^{-1}). This indicates that the polymeric Sb–O chains found in valentinite[7] are retained in the melt. Only small differences in frequencies and intensities are seen (probably due to thermal effects) in the internal mode region, suggesting that these spectral features of crystalline valentinite are mainly controlled by the polymeric Sb–O chains and only weakly controlled by the crystal space group and unit cell couplings. The Raman spectrum of the melt has also lost all the lattice mode bands, i.e., bands found below 400 cm^{-1} in crystalline valentinite.

When either form of Sb_2O_3 was heated in nitrogen, the condensate found in the cooler regions of the TG furnace was senarmontite. Thus, the vapors formed upon heating either senarmontite or valentinite do not contain polymeric Sb–O chains but must be instead discrete molecules. Previous studies have indicated that the gaseous product is the dimer of Sb_2O_3, i.e., Sb_4O_6.[15,16] Hence, it can be concluded that senarmontite is condensed when either form of Sb_2O_3 is volatilized. In hotter regions of the condensing apparatus, senarmontite would undergo a phase transformation to valentinite. Remy[1] reported the senarmontite to valentinite phase transformation occurs at 573 °C; White[17] et al. reported 610 °C as the transition temperature.

The sublimation temperature of α-Sb_2O_4 varies depending upon the preparation procedure and whether the sample is heated in air or nitrogen. For instance, sublimation of α-Sb_2O_4 commenced at 950 °C when the tetroxide was formed by heating $Sb_2O_5 \cdot XH_2O$ in N_2 at 50 °C/min. Thermolysis curves for α-Sb_2O_4, prepared from the oxidation of Sb_2O_3, when heated in air and N_2 at 20 °C/min from ambient to 1200 °C differ, with sublimation occurring at 1050 and 1000 °C, respectively. The variance in sublimation temperatures for these samples is probably a function of particle size, particle shape or surface area, and the heating rate. The condensate formed by either air or N_2 sublimation is a function of the

Table I. Vibrational Frequencies of Antimony Oxides

Formula Name	Raman Frequency (cm^{-1})	Raman (a) Intensity	Infrared (b) Frequency	Formula Name	Raman Frequency (cm^{-1})	Raman (a) Intensity	Infrared (b) Frequency
	84	26			71	14	
	124	8½			103	5	
Sb_2O_3	197	53		Sb_2O_3	140	100	
Senarmontite	261	100		Valentinite	194	15	
	364	<1			223	32½	
	381	7	675 sh		269	sh	
	458	13½	740		294	46	455
	722	2	960 w		449	7	488 sh
					502	24	540
					602	8	585 sh
					690	3	740
	43	30½					
	50	6					
	62	69					
	75	sh			79	58	
	78	11½			94	11½	
	91	3		β-Sb_2O_4	142	8½	
	101	<1			195	sh	
	137	sh			212	100	400 sh
	140	30½			283	1	420
α-Sb_2O_4	192	sh			405	24½	495 sh
	200	100			439	1	625 sh
Cervantite	209	sh			466	3½	655
	224	4			635	1½	715
	241	1½			754	<1	750 sh
	255	6½					
	263	16					
	274	<1					
	285	2					
	373	<1		$Sb_2O_5 \cdot x\,H_2O$	502 vb	100	435
	403	30			620 vb	10	740
	420	sh	421				850 sh
	455	sh					
	467	12½	528 v.w.				
	713	<1	605 sh				
	730	<1	650				430
	758	<1	745		420 vb	10 sh	555
	819	<1		Sb_6O_{13}	470 vb	100	720
	858	<1			550 vb	19 sh	760
							890 sh

a) Strongest band assigned intensity = 100

b) only recorded in the 1100 - 400 cm^{-1} interval

sh = shoulder; w = weak; v.w. = very weak; v.b. = very broad

collection temperature (see below) and was always found to be either senarmonitite, valentinite, or α-Sb_2O_4. These results suggest that the thermal decomposition products of α-Sb_2O_4 are gaseous Sb_2O_3 (or its dimer) and O_2. Senarmontite is condensed in the cooler regions of the furnace whereas valentinite is formed at moderate temperatures via the senarmontite–valentinite phase transition. In the hottest regions of the furnace, O_2 from the air and/or O_2 produced by the decomposition of α-Sb_2O_4 oxidizes the valentinite back to α-Sb_2O_4.

Rogers and Skapski[4] have suggested that β-Sb_2O_4 probably forms in the following manner:

$$2\alpha\text{-}Sb_2O_4(\text{solid}) \rightarrow Sb_4O_6(\text{vapor}) + O_2 \rightarrow 2\beta\text{-}Sb_2O_4(\text{solid})$$

To examine if β-Sb_2O_4 could be produced from α-Sb_2O_4 and oxygen, we held α-Sb_2O_4 between 1130 and 1180 °C in pure flowing O_2. Before sublimation was complete the reaction was stopped, and Raman spectra showed the residue was α-Sb_2O_4 with only a minor amount of β-Sb_2O_4 being detected. Examination of the condensate revealed it to be senarmontite. Production of β-Sb_2O_4 was achieved, however, by sealing α-Sb_2O_4 in quartz capillaries (at ambient air pressures) and then heating the capillaries to 960 °C. The α-$Sb_2O_4 \rightarrow \beta$-$Sb_2O_4$ phase transformation was very fast, requiring only a few minutes for ~100% conversion at this temperature.

The mechanism for $\alpha \rightarrow \beta$ conversion is still uncertain but would appear to be strongly influenced by the vapor pressure of the system. Waring et al.[9] have concluded that the β phase is the stable form of antimony tetroxide at very high pressure, a conclusion supported in part by the sealed capillary experiment. The pressure required for β formation was estimated to be approximately 5 atm in the present investigation, whereas Waring et al. indicated much higher pressures were necessary to complete the α- to β-Sb_2O_4 conversion. Knop[18] has suggested that minor impurities could substantially alter the $\alpha \rightarrow \beta$ formation dynamics. Further research must be carried out to evaluate both of these suggestions.

Heating β-Sb_2O_4 in air or N_2 atmosphere at 20 °C/min from ambient to 1200 °C shows the air-heated sample beginning to sublime at 1050 °C while the nitrogen-heated sample begins to sublime at 970 °C. The condensation product from these experiments was senarmontite, in the cooler regions of the furnace, for both atmospheres. The residues of the partially sublimed specimens were β-Sb_2O_4.

The thermolysis curve for $Sb_2O_5 \cdot XH_2O$ heated in air at 50 °C/min is given in Figure 1, trace e. The temperature boundaries of plateau regions are slightly different due to the heating rate; however, the general shape of the curve is similar to that reported by Stewart et al.[5] The final product of the present study was α-Sb_2O_4, and not β-Sb_2O_4, as reported by other researchers.[5] Stewart[5] prepared β-Sb_2O_4 by "firing" $Sb_2O_{4.35}$ (Sb_6O_{13}) in air above 935 °C. No additional experimental conditions were given. This information was used to infer that the product corresponding to the TG plateau above 930 °C is β-Sb_2O_4. Analysis of residues from TG experiments was not given. Residues from the present $Sb_2O_5 \cdot XH_2O$ TG runs were analyzed by Raman spectroscopy

Table II. Summary of Thermal Results

identification[a]	heating rate, °C/min	atmosphere at 100 cm³/min	reaction temp, °C[a]	residue	condensate
Sb_2O_3 Sen.	20	air	500–640 vol of Sen.	α-Sb_2O_4, 660–935 °C	Sen.[b] above 950 °C
Sb_2O_3 Sen.	20	N_2	500–750 vol of Sen.		
Sb_2O_3 Val.	20	air	500–560 vol of Val.	α-Sb_2O_4, 570–935 °C	Sen. above 950 °C
Sb_2O_3 Val.	20	N_2	500–790 vol of Val.		Sen.
α-Sb_2O_4	20	air	1050–onset[c] of vol	mostly α-Sb_2O_4; minor β-Sb_2O_4	Sen.[b] at 1195 °C
α-Sb_2O_4	20	N_2	1000–onset[c] of vol	α-Sb_2O_4	Sen.[b] at 1100 °C
β-Sb_2O_4	20	air	1050–onset of vol	β-Sb_2O_4 at 1200 °C	Sen. at 1200 °C
β-Sb_2O_4	20	N_2	970–onset of vol	β-Sb_2O_4 at 1130 °C	Sen. at 1130 °C
$Sb_2O_5 \cdot XH_2O$	50	air	650–850 Sb_6O_{13}	α-Sb_2O_4 890–970 °C	Sen. above 970 °C
$Sb_2O_5 \cdot XH_2O$	50	N_2	650–900 Sb_6O_{13}	α-Sb_2O_4, 950–onset of vol	Sen. above 950 °C

[a] Key: Sen. = senarmontite, Val. = valentinite, vol = volatilization. [b] Senarmontite found in cooler region of furnace, valentinite in the moderate temperature region and α-Sb_2O_4 in the hotter temperature zone. [c] Varies according to method of preparation and atmosphere employed. See text.

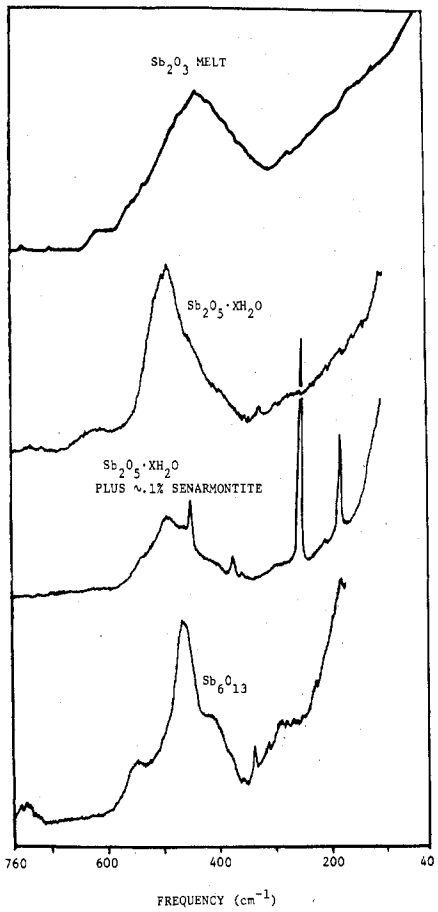

Figure 3. Raman spectra of Sb_2O_3 melt, polycrystalline $Sb_2O_5 \cdot XH_2O$, $Sb_2O_5 \cdot XH_2O$ with ~0.1% senarmontite, and Sb_6O_{13}. Spectra were recorded at 4 cm^{-1} resolution.

and X-ray diffraction. The residue corresponding to the TG plateau from 650 to 850 °C is Sb_6O_{13}. The residue corresponding to the 890–970 °C plateau is α-Sb_2O_4.

Heating $Sb_2O_5 \cdot XH_2O$ in N_2 produced a thermal curve similar to that seen in Figure 1, trace e. In a nitrogen atmosphere, however, as the Sb_6O_{13} converts to α-Sb_2O_4, the α-Sb_2O_4 is immediately volatilized, and the short plateau region from 890 to 970 °C is lost. The Raman spectrum of the residue after being partially volatilized confirmed the presence of pure α-Sb_2O_4. The condensate recovered in the cooler portion of the furnace was senarmontite. Table II summarizes all the thermal findings and results.

Cheremisinov[19] described the Raman spectrum of $Sb_2O_5 \cdot 5XH_2O$ as consisting of 16 bands falling between 58 and 1250 cm^{-1}; he assigned 13 bands as fundamentals. The Raman spectrum of $Sb_2O_5 \cdot XH_2O$ recorded during our study (Figure 3) consisted of a broad weak band centered at ~502 cm^{-1} with a broad very weak shoulder at ~620 cm^{-1}. Raman spectra recorded with different exciting lines were very reproducible, and, therefore, it could be concluded that the two weak broad features are the actual spectrum and are not due to fluorescent impurities or instrumental artifacts. The 502- and 620-cm^{-1} bands were also seen in spectra recorded from pressed pellets, ruling out capillary fluorescence. These spectral features have also been verified by an independent investigation.[20]

As a final check, the Raman spectrum of $Sb_2O_5 \cdot XH_2O$ mixed with ~0.1 wt % senarmontite was recorded (Figure 3). The bands at 197, 261, and 381 cm^{-1} are due to senarmontite while the weak broad $Sb_2O_5 \cdot XH_2O$ bands are still seen at ~502 and ~620 cm^{-1}.

These types of spectral features are usually associated with noncrystalline materials, i.e., amorphous, or materials having no first-order Raman spectrum. The suggestion that the spectrum is characteristic of an amorphous solid can be ruled out because the $Sb_2O_5 \cdot XH_2O$ produced a well-defined X-ray diffraction pattern with sharp peaks, an indication that the sample was crystalline. The X-ray pattern was reported to be consistent with O_h^7 symmetry, space group $Fd3m$.[5] Other compounds having similar high symmetry, for example $BaZrO_3$, have no first-order Raman spectrum.[21]

The thermal decomposition of $Sb_2O_5 \cdot XH_2O$ proceeds via the formation of Sb_6O_{13}, which is stable in the temperature range of 650–850 °C (Figure 1, trace e). There is no indication of a weight change when Sb_6O_{13} is heated from ambient to 890 °C in air at 20 °C/min. From 890 to 970 °C a 1.7% weight loss occurs. The residue was identified as α-Sb_2O_4. The X-ray diffraction patterns of Sb_6O_{13} indicated the material was crystalline, and again the high symmetry could have eliminated any first-order Raman spectrum, so that only a weak broad second-order spectrum was seen, Figure 3. $Sb_2O_5 \cdot XH_2O$ and Sb_6O_{13} can be distinguished by Raman spectroscopy, however, on the basis of position of the weak broad second-order feature seen in both spectra. For $Sb_2O_5 \cdot XH_2O$ the broad band is seen at ~502 cm^{-1} whereas this same feature is seen at ~460 cm^{-1} for Sb_6O_{13}.

Acknowledgment. We wish to thank E. A. Sedhom for recording and interpreting the X-ray diffraction patterns.

Registry No. Sb_2O_3, 1309-64-4; Sb_2O_4, 1332-81-6; Sb_2O_5, 1314-60-9; Sb_6O_{13}, 12165-47-8; sernarmontite, 12412-52-1; valentinite, 1317-98-2; cervantite, 12340-12-4.

References and Notes

(1) H. Remy, "Treatise on Inorganic Chemistry", Vol. II, Elsevier, New York, 1956, p 665.

(2) K. Dihlström, *Z. Anorg. Chem.*, **239**, 57 (1938).
(3) E. J. Roberts and F. Fenwick, *J. Am. Chem. Soc.*, **50**, 2125 (1928).
(4) D. Rogers and A. C. Skapski, *Proc. Chem. Soc., London*, 400 (1964).
(5) D. J. Stewart, O. Knop, C. Ayasse, and F. W. D. Woodhams, *Can. J. Chem.*, **50** 690 (1972).
(6) P. S. Gopalakrishnan and H. Manohar, *Curr. Sci.*, **38** (13), 306 (1969).
(7) P. S. Gopalakrishnan and H. Manohar, *J. Solid State Chem.*, **15**, 61 (1975); **16**, (1976).
(8) M. B. Varfolomeev, I. S. Shostak, M. N. Sotnikova and V. E. Plyushchev, *Izv. Akad. Nauk SSSR, Neorg. Mater.*, **11**, 962 (1975).
(9) J. L. Waring, R. S. Roth, H. S. Parker, and W. S. Brower, *Mater. Res. Bull.*, **80A**, 761 (1976).
(10) Y. K. Agrawal, A. L. Shushinohan, and A. B. Besivas, *J. Therm. Anal.*, 7, 635 (1975).
(11) Conditions used were particle sizes of 0.1–6 μm, heating rates of 5–20 °C/min, air flow rates of 100 and 200 mL/min, and sample sizes of 7–60 mg. Senarmontite was observed to lose 21–26 wt % during TG runs in air.
(12) O. Borgen and J. Krogh-Moe, *Acta Chem. Scand.*, **10**, 265 (1956).
(13) Z. M. Hanafi, K. A. Alzewel, E. M. H. Ibrahim, and M. M. Abou Sekkina, *Z. Phys. Chem. (Frankfurt am Main)*, **945**, 291 (1975).
(14) I. R. Beattie, K. M. S. Livingston, G. A. Ozin, and E. J. Reynolds, *J. Chem. Soc. A*, 449 (1970).
(15) P. A. Akishin and V. P. Spiridonov, *Zh. Strukt. Khim.*, **2**, 542 (1961).
(16) P. A. Akishin, L. V. Vilkov, E. Z. Zasarin, N. G. Rambidi, and V. P. Spiridonov, *J. Phys. Soc. Jpn.*, **17**, 18 (1962).
(17) W. B. White, F. Dachille, and R. Roy, *Z. Kirstallogr., Kristallegom., Kristallphys., Kristallchem.*, **125**, 450 (1967).
(18) Private communication with O. Knop, Dalhousie University.
(19) V. P. Cheremisinov, *Tr. Fiz. Inst., Akad. Nauk SSSR*, **25**, 153 (1964).
(20) Private communication with J. Nestor, Princeton University.
(21) A. E. Pasto and R. A. Condrate, Sr., *Adv. Raman Spectrosc.*, **1** (1973).

Contribution from the Radiation Laboratory,
University of Notre Dame, Notre Dame, Indiana 46556

Photochemical Properties of the Low-Spin Iron(II)–2,3,9,10-Tetramethyl-1,4,8,11-tetraazacyclotetradeca-1,3,8,10-tetraene Complexes. An Investigation of the Secondary Thermal Substitution Reactions by Laser and Flash Photolysis

G. FERRAUDI

Received September 8, 1978

The photochemical properties of the Fe(II)–TIM (TIM = 2,3,9,10-tetramethyl-1,4,8,11-tetraazacyclotetradeca-1,3,-8,10-tetraene) complexes have been investigated by laser and flash photolysis. Rapid substitution reactions of the metastable products have been observed in photolyses of $Fe(TIM)(NCS)_2$, $Fe(TIM)(imid)_2^{2+}$, and $Fe(TIM)(CH_3CN)(CO)^{2+}$ in acetonitrile. Also, photolysis induces a transient linkage isomerization of the thiocyanate complex and two photolabilization processes, substitution of CO and CH_3CN, in $Fe(TIM)(CH_3CN)(CO)^{2+}$. A precursor, assigned as pentacoordinated $Fe(TIM)(CO)^{2+}$, was detected in laser flash photolysis. Aspects of the photosubstituion processes in Fe(II)–TIM complexes are discussed.

Introduction

Photosubstitution reactions of the low-spin iron(II) complexes of the macrocyclic TIM ligand[1] have been recently investigated by several authors.[2-5] The nature of the reactive excited state, charge-transfer metal to ligand (CTTL) or ligand field (LF), has been discussed in these studies. In this regard, the photochemical reactivity has been attributed to the population of LF states.[3]

The photolabilization of the ligand is controlled by the solvent.[4] However, the effect that anation of reactive products and intermediates may have upon the product yields has not been investigated. Processes of this kind, anation of metastable species, have been described for photochemical[6-8] and thermal substitutions[9,10] in low-spin cobalt(III) complexes. Moreover, photodissociative and photointerchange mechanisms have been proposed for the photolabilization reactions of the hexacyano and acidopentacyanocobalt(III) complexes.[5-8] In this regard, one may expect some points in common between the photochemical behavior of the low-spin cobalt(III) compounds, complexed with ligands of a large ligand field strength, and isoelectronic iron(II)–macrocyclic species.

Results on the photochemical and thermal secondary reactions of Fe(II)–TIM[1] complexes, investigated by laser and flash photolysis, are reported here.

Experimental Section

Photochemical Procedures. A description of the flash photolysis apparatus was given elsewhere.[11,12] Reactions of the intermediates were investigated by using various concentrations of these species. Different concentrations were produced with flash outputs which corresponded to stored electrical energies between 250 J/flash and 40 J/flash. Cutoff filters, transmissions at wavelengths $\lambda \geq 320$ nm and $\lambda \geq 410$ nm, were used for irradiations of the photolyte in preselected regions.

The laser flash photolysis apparatus was described in detail by Scaiano et al.[13] The directions of the monitoring and excitation beams were adjusted in order to obtain a tight overlap over the 2 mm optical path of the reaction cell. The monitoring pulse had a useful length of a few microseconds. The laser pulse, placed at the beginning of the monitoring interval, had a full width of 20 ns.

Solutions of the complexes were prepared by addition of a given amount of the solid compounds[14] to solvents which were previously deaerated with streams of argon. Also, $Fe(TIM)(CH_3CN)(CO)^{2+}$ was flash irradiated in solutions that were saturated under a given partial pressure of carbon monoxide. The solvent, in these experiments, was first freed of dioxygen with argon streams and was second equilibrated under a mixture of argon and carbon monoxide for 2 h. The ionic strength of the solutions was adjusted to 0.1 M with $NaClO_4$.

The experimental setup, used in continuous wave irradiations, was described in previous reports.[15] Light intensities, 10^{-4}–10^{-5} einstein/(L min), were measured with ferric oxalate[16] or Reinecke salt.[17]

Materials. The complexes $[Fe(TIM)(CH_3CN)_2](PF_6)_2$, $[Fe(TIM)(imid)_2](PF_6)_2$, and $[Fe(TIM)(CH_3CN)(CO)](PF_6)_2$ were obtained by reported procedures.[18] The purity of these complexes was investigated by comparison of their spectra with those reported by other authors.[2,18] These salts were converted into perchlorates by precipitation with solid $NaClO_4$ from acetonitrile or solutions with an excess of the ligands CO or imidazole in acetonitrile.

$[Fe(TIM)(NH_3)_2](PF_6)_2$ was prepared by the method of Incorvia and Zink.[2] A modification of this procedure was used for the synthesis of the $[Fe(TIM)(N(C_2H_5)_3)_2](PF_6)_2$. Indeed, the dry ammonia gas was replaced by addition of triethylamine, in a fivefold excess of the stoichiometric amount, to a solution of the bis(acetonitrile) complex in CH_2Cl_2. This solution was slowly evaporated with streams of argon.

Anal. Calcd for $FeC_{26}N_6H_{54}P_2F_6$: C, 45.87; H, 8.00. Found: C, 45.91; H, 7.99.

$[Fe(TIM)(NCS)_2]$, the bis(acetonitrile) complex (1 g), was dissolved in the minimum amount of deaerated methanol.[19] NaNCS (0.1 g), dissolved in deaerated methanol, was added. The greenish blue precipitate was filtered and dried in vacuo. The air oxidation of the Fe(II) complexes in methanolic solutions was prevented by

0020-1669/79/1318-1576$01.00/0